H_∞ Load Frequency Control Design Based on Delay Discretization Approach for Interconnected Power Systems with Time Delay

Subrat Kumar Pradhan and Dushmanta Kumar Das

Abstract—**This paper proposes a delay discretization based H_∞ load frequency control strategy for interconnected power systems. The effect of time delay is considered in the system for the design of stabilizing controller. To improve the tolerable delay margin of the system, a two-term state feedback controller structure is used. The controller requires delayed state information as control input. In the proposed approach, the amount of delay introduced in the state of the system, i.e., artificial delay, for taking control action is assumed to be constant. The approach is based on the discretization of this delay interval. In order to define a simple Lyapunov-Krasovskii (LK) function for each of the discretized interval, a stabilization criterion is developed in such a way that a single one satisfies the requirement of all the intervals. The developed criterion is computationally simple and efficient.**

Index Terms—**Interconnected power system, load frequency control (LFC), state feedback controller, time delay.**

I. Introduction

In a large-scale power system, multiple control areas are connected through tie-lines. For supplying reliable and sufficient power of good quality, one of the most important components of the large-scale power system is the load frequency control (LFC) [1]. In LFC, the balance between power generation and demand needs to be satisfied. For LFC, some requirements must be taken into account such as: ① the minimization of the steady state error of tie-line exchanges and frequency deviations [2]; ② the optimal transient behavior [3]; ③ the optimal power dispatch [4], [5]. For interconnected power system, area control error (ACE) signal is used as an input for automatic regulation of frequency deviation [6]. And dedicated communication channels are used for the transmission of measured data from remote terminal units (RTUs) to the control center, and ACE signal from the control center to the generation station [7], [8]. During the modeling of interconnected power systems, it is unable to avoid the time required to collect the information of load frequency deviation by regulation station, and generate and transmit ACE signal from regulation station to different power system areas. This time lag or time delay in the system model makes the system dynamics infinite dimensional (infinite number of roots of the characteristics polynomial) [9]. The design of control algorithm is always a challenging task for such systems. This time delay in ACE signal may lead to oscillation and instability in power systems [10], [11]. For a reliable interconnected power system, the controller is to be designed without neglecting the delay factor in the system. Therefore, a delay-dependent stabilization criterion should be developed so that the maximum tolerable delay margin (MTDM) of an LFC scheme can be improved [10]-[13].

There has been available literature on designing suitable controllers for LFC scheme of an interconnected power system. One of the simplest controller, i.e., a proportional-integral (PI) control, is proposed in [5], [6]. To achieve better performance, some controllers such as H_∞ controller [14] and adaptive controller [4] are proposed. In [15], the effect of time-delay on LFC of microgrid is studied and a method is proposed to compute the delay margin. Various advanced control strategies are also proposed such as robust control design technique [16]-[18], H_∞ based decentralized control design [19], [20] and sliding mode control [21]. However, most of the advanced control strategies suggest nonlinear, complex state feedback and higher-order dynamic controllers. In fact, due to simple structure and effectiveness, simple state feedback and proportional-integral-derivative (PID) controllers are still preferred in industrial applications. To tune the controller gains, many methods are available such as fuzzy based tuning [22] and linear matrix inequality (LMI) based approach [10], [23]. In [12], a decentralized control strategy using two-term controller is proposed for the LFC problem. Though there are a number of control techniques available in literature to design a controller, H_∞ control technique is a very popular control technique for controller design. The H_∞ controller in a control system has some advantages such as: ① it achieves stabilization with guaranteed performance [24]; ② it increases the robustness against uncertainties [25]; and ③ it restrains interferences, unmodeled dynamics or both of them [26]. In [9]-[11], a logic of introducing an artificial delay in the state of the controller is proposed, which improves the tolerable delay margin of the closed loop system. Specifically, for LFC scheme, a two-

Manuscript received: April 3, 2019; accepted: February 27, 2020. Date of CrossCheck: February 27, 2020. Date of online publication: August 7, 2020.

S. K. Pradhan and D. K. Das (corresponding author) are with the Department of Electrical and Electronics Engineering, National Institute of Technology Nagaland, Dimapur 797103, India (e-mail: subrat.pradhan48@gmail.com; dushmantakumardas29@gmail.com).

DOI: 10.35833/MPCE.2019.000206

term state feedback controller is used in [10], [11], [27] to derive the stabilization criterion and to satisfy the H_∞ performance criterion. The logic behind the use of this artificial delay in the state of the controller is that the controller dynamics involves the delayed state information of the time-delay system. This improves the tolerable delay margin of the time-delay system.

In this paper, the LFC problem of interconnected power system with delay in ACE is analysed by using delay-discretization approach. H_∞ performance based delayed state feedback control strategy is proposed by using an artificial delay for tolerable delay margin enhancement of the interconnected power system. The artificial delay is chosen for discretization because it incorporates the delayed state information of interconnected power system into the dynamics of the controller, which is the primary requirement of the proposed control method. The number of decision variables increases with the number of delay intervals in the existing delay discretization approaches [28]-[31]. However, the proposed delay discretization approach with discretization of artificial delay is computationally simple and efficient as the number of decision variables does not increase with the number of delay intervals. A new multiple Lyapunov-Krasovskii (LK) function based approach is proposed to derive an improved H_∞ based delay-dependent stabilization criterion for the interconnected power system. To derive the criterion, a simple LK function is defined for an arbitrary number of discretized delay intervals. The criterion for the highest interval is able to satisfy the stability requirement of all intervals and lead to a single criterion. Therefore, the number of decision variable does not change with the number of delay intervals. Hence, the computation time is reduced. To demonstrate the effectiveness of the criterion, a well-known numerical example is considered in [10].

The contributions of this paper are listed as follows.

1) It deals with the effect of time delay related to ACE on the LFC problem of an interconnected power system.

2) A state feedback H_∞ controller containing both present and delayed state information is designed to improve tolerable delay margin of the interconnected power system.

3) By using delay-discretization approach, a new stabilization criterion with H_∞ performance index is derived in terms of LMI based on LK function for interconnected power system with time delay.

4) To compute suitable controller gains and H_∞ performance index, a constrained LMI optimization problem is developed by formulating a multi-objective function.

5) A study is conducted to show the effect of the number of delay intervals on tolerable delay margin of the interconnected power system.

II. System Description and Preliminaries

There are different types of LFC structures in regulated and deregulated power markets. In this paper, charged LFC structure is considered. For simple understanding, a charged LFC structure of two-area interconnected power system is shown in Fig. 1. In this scheme, the transmission companies (TRANSCOs) purchase power from generation companies (GENCOs) and sell it to distribution companies (DISCOs). The TRANSCOs have the responsibility of measuring the load frequency deviation and net tie-line power deviation, and generate control signal to GENCOs to adjust the real output power. In an interconnected power system, delays are present in the i^{th} area power system in ACE due to the following reasons: ① time taken in measuring/sensing the frequency deviation and tie-line power; ② time taken in transmitting the sensor data to controller and control signal from the controller to generation station. Therefore, it is wiser to consider the effect of delays in the system dynamics at the time of controller design such that an appropriate controller can be designed to withstand the effect of total closed loop delay with larger margin.

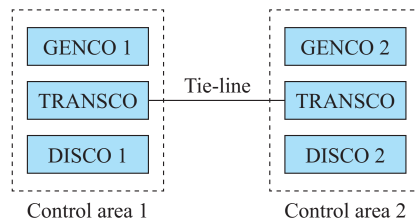

Fig. 1. Charged LFC structure without bilateral contract.

The LFC model of the i^{th} area power system with time delay in ACE is shown in Fig. 2, where ΔP_{vi} is the governor valve position deviation of area i; ΔP_{mi} is the mechanical output power deviation of area i; Δf_i is the frequency deviation of area i; ΔE_i is the ACE of area i; ΔP_{ij} is the tie-line power deviation of areas i and j; ΔP_{di} is the load disturbance of area i; T_{gi} is the governor time constant of area i; T_{pi} is the time constant of power system of area i; T_{chi} is the time constant of turbine of area i; T_{ij} is the stiffness coefficient between areas i and j; k_{pi} is the proportional gain of PI controller of area i; k_i is the integral gain of PI controller of area i; B_i is the frequency bias parameter of area i; R_i is the speed droop of area i; τ_i is the time delay in ACE of area i; and u_i is the control input to area i.

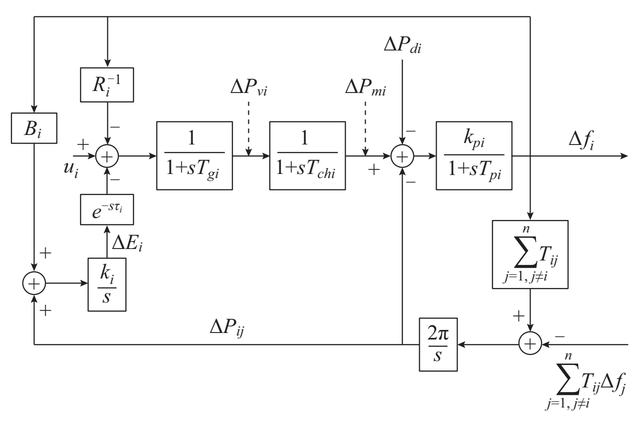

Fig. 2. LFC model of the i^{th} control area in an interconnected power system with time delay.

The objective of this paper is to design a suitable controller to stabilize the closed loop system, which, at the same time, can ascertain the H_∞ performance criterion. The H_∞ performance index Γ is described as:

$$\left\| T_{wy}(\mathrm{j}\omega) \right\| \le \Gamma \quad \forall \omega \tag{1}$$

where $T_{wy}(\mathrm{j}\omega)=T_{wy}(s)=L\left(\dfrac{\boldsymbol{y}(t)}{\boldsymbol{w}(t)}\right)$, L is the Laplace operator, $\boldsymbol{w}(t)$ is disturbance vector, $\boldsymbol{y}(t)$ is the output vector; and ω is the frequency domain function. Equation (1) can be defined as:

$$\left\| T_{wy} \right\|_\infty = \frac{\left\| \boldsymbol{y} \right\|_2}{\left\| \boldsymbol{w} \right\|_2} = \frac{\sqrt{\int_0^\infty \boldsymbol{y}^{\mathrm{T}}(t)\boldsymbol{y}(t)\mathrm{d}t}}{\sqrt{\int_0^\infty \boldsymbol{w}^{\mathrm{T}}(t)\boldsymbol{w}(t)\mathrm{d}t}} \le \Gamma \tag{2}$$

where the H_∞ performance index Γ is the load rejection ratio of the controller. It is required to obtain an H_∞ controller to minimize Γ, i.e., norm bounded performance measure, in order to have the minimal effect of load variation on the performance of system.

The dynamics of an interconnected power system with n control areas for $i,j=1,2,...,n, i\ne j$ can be described as follows.

The linearized model of the alternator output mechanical power deviation is given by:

$$\Delta \dot{P}_{mi}(t) = \frac{\Delta P_{vi}(t)}{T_{chi}} - \frac{\Delta P_{mi}(t)}{T_{chi}} \tag{3}$$

The linearized model of ACE is given by:

$$\Delta \dot{E}_i(t) = k_i \Delta P_{ij}(t) + k_i B_i \Delta f_i(t) \tag{4}$$

The linearized model of the tie-line power deviation is given by:

$$\Delta \dot{P}_{ij}(t) = 2\pi T_{ij}\Delta f_i(t) - 2\pi T_{ij}\Delta f_j(t) \tag{5}$$

The linearized model of the governor valve position is given by:

$$\Delta \dot{P}_{vi}(t) = -\frac{\Delta f_i(t)}{R_i T_{gi}} - \frac{\Delta P_{vi}(t)}{T_{gi}} - \frac{\Delta E_i(t-\tau_i)}{T_{gi}} + \frac{u_i(t)}{T_{gi}} \tag{6}$$

The linearized model of frequency deviation is given by:

$$\Delta \dot{f}_i(t) = -\frac{k_{pi}}{T_{pi}}\left(\Delta P_{di}(t) + \Delta P_{ij}(t) - \Delta P_{mi}(t)\right) - \frac{\Delta f_i(t)}{T_{pi}} \tag{7}$$

where $\Delta P_{ij} = -\Delta P_{ji}$.

The dynamic equations (3)-(7) collectively describe the generalized dynamic model of multi-area interconnected power system for LFC analysis. One can analyse the LFC problem of an interconnected power system containing any number of control areas by using this dynamic model. In this dynamic model, the number of parameters increases with n, i.e., incorporation of more control areas into the interconnected power system increases the number of system parameters. Thus, for convenience, by choosing $n=2$, a two-area interconnected power system containing ACE delay in both control areas is considered for LFC analysis in this paper. The dynamic model of the two-area interconnected power system can be obtained from (3)-(7) for $i,j=1,2, i\ne j$. The two-area LFC model is shown in Fig. 3, which is modeled following Fig. 2.

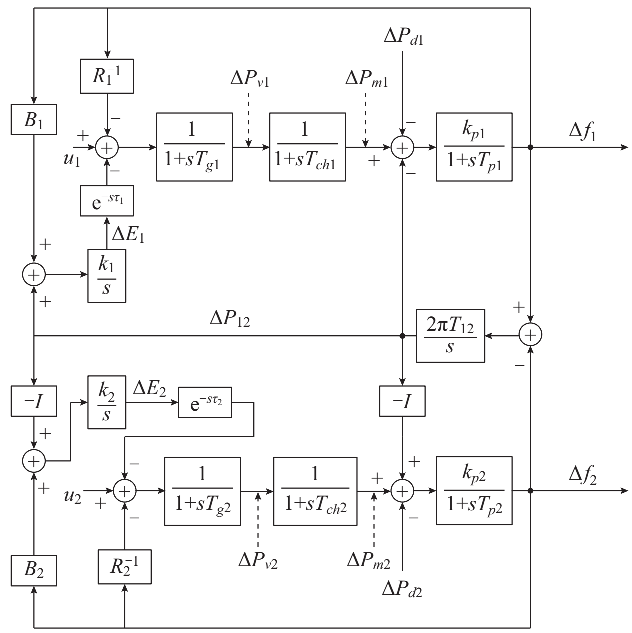

Fig. 3. Two-area LFC model.

Define a state vector as $\boldsymbol{x}(t)=\left[\Delta \boldsymbol{A}_{r1}\ \ \Delta P_{12}\ \ \Delta \boldsymbol{A}_{r2}\right]^{\mathrm{T}}$, where $\Delta \boldsymbol{A}_{r1}=\left[\Delta f_1\ \Delta P_{m1}\ \Delta P_{v1}\ \Delta E_1\right]$, $\Delta \boldsymbol{A}_{r2}=\left[\Delta f_2\ \Delta P_{m2}\ \Delta P_{v2}\ \Delta E_2\right]$. The dynamic equations (3)-(7) for the two-area LFC can be represented in a state-space form as:

$$\dot{\boldsymbol{x}}(t) = \boldsymbol{A}\boldsymbol{x}(t) + \boldsymbol{A}_{d1}\boldsymbol{x}(t-\tau_1) + \boldsymbol{A}_{d2}\boldsymbol{x}(t-\tau_2) + \boldsymbol{B}\boldsymbol{u}(t) + \boldsymbol{D}\boldsymbol{w}(t) \tag{8}$$

$$\boldsymbol{y}(t) = \boldsymbol{C}\boldsymbol{x}(t) \tag{9}$$

where $\boldsymbol{w}(t)=\Delta \boldsymbol{P}_d=[\Delta P_{d1}\ \ \Delta P_{d2}]^{\mathrm{T}}$ is the load disturbance vector. For $b=1,2$ and $l=3,4$, the following matrices are defined as:

$$\boldsymbol{A} = \begin{bmatrix} \boldsymbol{A}_1 & \boldsymbol{A}_3 & \boldsymbol{0}_{4\times 4} \\ \boldsymbol{A}_5 & \boldsymbol{0}_{1\times 1} & -\boldsymbol{A}_5 \\ \boldsymbol{0}_{4\times 4} & \boldsymbol{A}_4 & \boldsymbol{A}_2 \end{bmatrix} \tag{10}$$

$$\boldsymbol{A}_b = \begin{bmatrix} -\dfrac{1}{T_{pb}} & \dfrac{k_{pb}}{T_{pb}} & 0 & 0 \\ 0 & -\dfrac{1}{T_{chb}} & \dfrac{1}{T_{chb}} & 0 \\ -\dfrac{1}{R_b T_{gb}} & 0 & -\dfrac{1}{T_{gb}} & 0 \\ k_b B_b & 0 & 0 & 0 \end{bmatrix} \tag{11}$$

$$\boldsymbol{A}_l = \begin{bmatrix} -\dfrac{k_{pb}}{T_{pb}} & 0 & 0 & k_b \end{bmatrix}^{\mathrm{T}} \tag{12}$$

$$\boldsymbol{A}_5 = \begin{bmatrix} 2\pi T_1 & 0 & 0 & 0 \end{bmatrix} \tag{13}$$

$$\boldsymbol{A}_{d1} = \begin{bmatrix} \boldsymbol{0}_{4\times 3} & -\boldsymbol{A}_{d11} & \boldsymbol{0}_{4\times 5} \\ \boldsymbol{0}_{5\times 3} & \boldsymbol{0}_{5\times 1} & \boldsymbol{0}_{5\times 5} \end{bmatrix} \tag{14}$$

$$\boldsymbol{A}_{d2} = \begin{bmatrix} \boldsymbol{0}_{5\times 8} & \boldsymbol{0}_{5\times 1} \\ \boldsymbol{0}_{4\times 8} & -\boldsymbol{A}_{d21} \end{bmatrix} \tag{15}$$

$$\boldsymbol{A}_{db1} = \begin{bmatrix} 0 & 0 & \dfrac{1}{T_{gb}} & 0 \end{bmatrix}^{\mathrm{T}} \tag{16}$$

$$\boldsymbol{B} = \begin{bmatrix} \boldsymbol{A}_{d11} & \boldsymbol{0}_{4\times 1} \\ \boldsymbol{0}_{1\times 1} & \boldsymbol{0}_{1\times 1} \\ \boldsymbol{0}_{4\times 1} & \boldsymbol{A}_{d21} \end{bmatrix} \tag{17}$$

$$\boldsymbol{C} = \begin{bmatrix} \boldsymbol{C}_1 & \boldsymbol{0}_{4\times 1} \\ \boldsymbol{0}_{1\times 1} & \boldsymbol{0}_{1\times 1} \\ \boldsymbol{0}_{4\times 4} & \boldsymbol{C}_1 \end{bmatrix}^{\mathrm{T}} \tag{18}$$

$$\boldsymbol{C}_1 = \begin{bmatrix} I & 0 & 0 & 0 \end{bmatrix}^{\mathrm{T}} \tag{19}$$

$$\boldsymbol{D} = \begin{bmatrix} -\boldsymbol{D}_1 & \boldsymbol{0}_{4\times 1} \\ \boldsymbol{0}_{1\times 1} & \boldsymbol{0}_{1\times 1} \\ \boldsymbol{0}_{4\times 1} & -\boldsymbol{D}_2 \end{bmatrix} \tag{20}$$

$$\boldsymbol{D}_b = \begin{bmatrix} \dfrac{k_{pb}}{T_{pb}} & 0 & 0 & 0 \end{bmatrix}^{\mathrm{T}} \tag{21}$$

It can be noted that the local PI controller is considered as an integral part of the model (3)-(7). As the margin of delay τ_i increases, the local PI controller fails to stabilize the system in conventional LFC scheme. For such situation, the conventional PI controller may not improve the performance of the system [10], [32]. Therefore, a proper optimal control strategy may be designed to improve the performance of the system.

In [10], a single-term controller and a two-term controller with time delay have been considered. It is shown that the same approach to obtain the stabilization criterion using the two-term controller with delay structure is less conservative than the single-term controller. In [9], [27], it is also presented that the maximum tolerable delay margin of system can be improved by introducing artificial delays in the controller dynamics. Therefore, to obtain a less conservative criterion, the following steps are taken. The steps are described as follows.

1) To solve the LFC problem of time-delay power system, a two-term controller of the following form is proposed as:

$$\boldsymbol{u}(t) = \boldsymbol{K}\boldsymbol{x}(t) + \boldsymbol{K}_h\boldsymbol{x}(t-h) \tag{22}$$

where $\boldsymbol{K}$ and $\boldsymbol{K}_h$ are the controller gain matrices with satisfactory dimension; h is a known finite delay intentionally introduced in the controller by the designer (artificial delay or controller delay). Assume that h is a constant delay satisfying $0 \le h \le \bar{h}$, where $\bar{h}$ is the upper bound of h. The control signal generated for the system is a function of present and delayed state of the system.

2) To obtain the stabilization criterion using LK function in LMI framework, a discretization approach is proposed. Systems (8) and (9) are considered to validate the proposed control algorithm in this paper.

Using a controller of the form (22), the closed-loop system can be represented as:

$$\dot{\boldsymbol{x}}(t) = \boldsymbol{A}_c\boldsymbol{x}(t) + \boldsymbol{B}_h\boldsymbol{x}(t-h) + \boldsymbol{A}_{d1}\boldsymbol{x}(t-\tau_1) + \boldsymbol{A}_{d2}\boldsymbol{x}(t-\tau_2) + \boldsymbol{D}\boldsymbol{w}(t) \tag{23}$$

$$\boldsymbol{y}(t) = \boldsymbol{C}\boldsymbol{x}(t) \tag{24}$$

where $\boldsymbol{A}_c = \boldsymbol{A} + \boldsymbol{B}\boldsymbol{K}$ and $\boldsymbol{B}_h = \boldsymbol{B}\boldsymbol{K}_h$.

To derive the main stabilization criterion, an existing result is given in the form of Lemma which is discussed as follows.

Lemma 1 (Jensen's Inequality [33]): for any constant matrix $\boldsymbol{R} > \boldsymbol{0}$, $\beta > \alpha > 0$ and $\gamma = \beta - \alpha > 0$, the following bounding inequality holds:

$$-\int_{t-\beta}^{t-\alpha} \dot{\boldsymbol{x}}^{\mathrm{T}}(\theta)\boldsymbol{R}\dot{\boldsymbol{x}}(\theta)\mathrm{d}\theta \le \bar{\gamma} \begin{bmatrix} \boldsymbol{x}(t-\alpha) \\ \boldsymbol{x}(t-\beta) \end{bmatrix}^{\mathrm{T}} \begin{bmatrix} -\boldsymbol{R} & \boldsymbol{R} \\ \boldsymbol{R}^{\mathrm{T}} & -\boldsymbol{R} \end{bmatrix} \begin{bmatrix} \boldsymbol{x}(t-\alpha) \\ \boldsymbol{x}(t-\beta) \end{bmatrix} \tag{25}$$

where $\bar{\gamma} = \gamma^{-1}$. The right-hand side of the above inequality is nonconvex in γ. To approximate a convex criterion involving the uncertain parameter γ, an equivalent representation can be obtained using the free matrix variable. The approximated representation is as follows:

$$-\int_{t-\beta}^{t-\alpha} \dot{\boldsymbol{x}}^{\mathrm{T}}(\theta)\boldsymbol{R}\dot{\boldsymbol{x}}(\theta)\mathrm{d}\theta \le \begin{bmatrix} \boldsymbol{x}(t-\alpha) \\ \boldsymbol{x}(t-\beta) \end{bmatrix}^{\mathrm{T}} \left\{ \begin{bmatrix} \boldsymbol{M}+\boldsymbol{M}^{\mathrm{T}} & -\boldsymbol{M}+\boldsymbol{N}^{\mathrm{T}} \\ (-\boldsymbol{M}+\boldsymbol{N}^{\mathrm{T}})^{\mathrm{T}} & -\boldsymbol{N}-\boldsymbol{N}^{\mathrm{T}} \end{bmatrix} + \gamma \begin{bmatrix} \boldsymbol{M} \\ \boldsymbol{N} \end{bmatrix} \boldsymbol{R}^{-1} \begin{bmatrix} \boldsymbol{M} \\ \boldsymbol{N} \end{bmatrix}^{\mathrm{T}} \right\} \begin{bmatrix} \boldsymbol{x}(t-\alpha) \\ \boldsymbol{x}(t-\beta) \end{bmatrix} \tag{26}$$

where $\boldsymbol{M}$ and $\boldsymbol{N}$ are free weighted matrices with appropriate dimensions. Note that, with the choice $\boldsymbol{M} = \boldsymbol{M}^{\mathrm{T}} = -\boldsymbol{N} = -\boldsymbol{N}^{\mathrm{T}} = -\gamma^{-1}\boldsymbol{R}$ in (26), we can obtain (25).

III. Design of Delay-dependent H_∞ Two-term Controller

The following theorem presents an LMI-based criterion for designing the controller of form (22) while ascertaining the H_∞ performance criterion (2).

Theorem 1: system (8) with controller (22) for known α, β, λ and γ satisfies the H_∞ performance (2) if there exists $\bar{\boldsymbol{P}} > \boldsymbol{0}$, $\bar{\boldsymbol{Q}}_i > \boldsymbol{0}$, $\bar{\boldsymbol{Q}}_{hk} > \boldsymbol{0}$, $\bar{\boldsymbol{R}}_{\tau i} > \boldsymbol{0}$, $\bar{\boldsymbol{R}}_{hi} > \boldsymbol{0}$ for $k = 1, 2, 3, 4$, and arbitrary matrices $\bar{\boldsymbol{S}}_1$, $\bar{\boldsymbol{M}}_{hi} > \boldsymbol{0}$, $\bar{\boldsymbol{N}}_{hi} > \boldsymbol{0}$, $\boldsymbol{Y}$ and $\boldsymbol{V}$ for $i = 1, 2$, satisfying the following LMI:

$$\begin{bmatrix} \bar{\boldsymbol{\Theta}} & \delta\bar{\boldsymbol{\Phi}}_j \\ (\delta\bar{\boldsymbol{\Phi}}_j)^{\mathrm{T}} & -\bar{\boldsymbol{R}}_{h2} \end{bmatrix} < \boldsymbol{0} \quad j = 1, 2 \tag{27}$$

where $\bar{\boldsymbol{\Phi}}_1 = [\boldsymbol{0}, \boldsymbol{0}, \boldsymbol{0}, \bar{\boldsymbol{M}}_{h1}^{\mathrm{T}}, \bar{\boldsymbol{N}}_{h1}^{\mathrm{T}}, \boldsymbol{0}, \boldsymbol{0}, \boldsymbol{0}, \boldsymbol{0}]^{\mathrm{T}}$, $\bar{\boldsymbol{\Phi}}_2 = [\boldsymbol{0}, \boldsymbol{0}, \boldsymbol{0}, \boldsymbol{0}, \bar{\boldsymbol{M}}_{h2}^{\mathrm{T}}, \bar{\boldsymbol{N}}_{h2}^{\mathrm{T}}, \boldsymbol{0}, \boldsymbol{0}, \boldsymbol{0}]^{\mathrm{T}}$, $\bar{\boldsymbol{\Theta}} = [\bar{\boldsymbol{\Theta}}_{ij}]_{i,j=1,2,\ldots,9}$, $\bar{\boldsymbol{\Theta}}_{11} = \boldsymbol{A}\bar{\boldsymbol{S}}_1^{\mathrm{T}} + \bar{\boldsymbol{S}}_1\boldsymbol{A}^{\mathrm{T}} + \boldsymbol{B}\boldsymbol{Y} + \boldsymbol{Y}^{\mathrm{T}}\boldsymbol{B}^{\mathrm{T}} + \sum_{k=1}^{2}\bar{\boldsymbol{Q}}_k - \bar{\boldsymbol{R}}_{h1} - \bar{\boldsymbol{R}}_{\tau_1} - \bar{\boldsymbol{R}}_{\tau_2} + \sum_{k=1}^{3}\bar{\boldsymbol{Q}}_{hk}$, $\bar{\boldsymbol{\Theta}}_{12} = \boldsymbol{A}_{d1}\bar{\boldsymbol{S}}_1^{\mathrm{T}} + \bar{\boldsymbol{R}}_{\tau_1}$, $\bar{\boldsymbol{\Theta}}_{13} = \boldsymbol{A}_{d2} \cdot \bar{\boldsymbol{S}}_1^{\mathrm{T}} + \bar{\boldsymbol{R}}_{\tau_2}$, $\bar{\boldsymbol{\Theta}}_{14} = \lambda\bar{\boldsymbol{S}}_1\boldsymbol{A}^{\mathrm{T}} + \lambda\boldsymbol{Y}^{\mathrm{T}}\boldsymbol{B}^{\mathrm{T}} + \bar{\boldsymbol{R}}_{h1}$, $\bar{\boldsymbol{\Theta}}_{15} = \beta\bar{\boldsymbol{S}}_1\boldsymbol{A}^{\mathrm{T}} + \beta\boldsymbol{Y}^{\mathrm{T}}\boldsymbol{B}^{\mathrm{T}} + \boldsymbol{B}\boldsymbol{V}$, $\bar{\boldsymbol{\Theta}}_{16} = \gamma\bar{\boldsymbol{S}}_1\boldsymbol{A}^{\mathrm{T}} + \gamma\boldsymbol{Y}^{\mathrm{T}}\boldsymbol{B}^{\mathrm{T}}$, $\bar{\boldsymbol{\Theta}}_{17} = -\bar{\boldsymbol{S}}_1^{\mathrm{T}} + \alpha\bar{\boldsymbol{S}}_1\boldsymbol{A}^{\boldsymbol{T}} + \alpha\boldsymbol{Y}^{\boldsymbol{T}}\boldsymbol{B}^{\boldsymbol{T}} + \bar{\boldsymbol{P}}$, $\bar{\boldsymbol{\Theta}}_{18} = \boldsymbol{D}$, $\bar{\boldsymbol{\Theta}}_{19} = \bar{\boldsymbol{S}}_1\boldsymbol{C}^{\mathrm{T}}$, $\bar{\boldsymbol{\Theta}}_{22} = -\bar{\boldsymbol{Q}}_1 - \bar{\boldsymbol{R}}_{\tau_1}$, $\bar{\boldsymbol{\Theta}}_{24} = \lambda\bar{\boldsymbol{S}}_1\boldsymbol{A}_{d1}^{\mathrm{T}}$ $\bar{\boldsymbol{\Theta}}_{25} = \beta\bar{\boldsymbol{S}}_1\boldsymbol{A}_{d1}^{\mathrm{T}}$, $\bar{\boldsymbol{\Theta}}_{26} = \gamma\bar{\boldsymbol{S}}_1\boldsymbol{A}_{d1}^{\mathrm{T}}$, $\bar{\boldsymbol{\Theta}}_{27} = \alpha\bar{\boldsymbol{S}}_1\boldsymbol{A}_{d1}^{\mathrm{T}}$, $\bar{\boldsymbol{\Theta}}_{33} = -\bar{\boldsymbol{Q}}_2 - \bar{\boldsymbol{R}}_{\tau_2}$, $\bar{\boldsymbol{\Theta}}_{34} = \lambda\bar{\boldsymbol{S}}_1\boldsymbol{A}_{d2}^{\mathrm{T}}$, $\bar{\boldsymbol{\Theta}}_{35} = \beta\bar{\boldsymbol{S}}_1\boldsymbol{A}_{d2}^{\boldsymbol{T}}$, $\bar{\boldsymbol{\Theta}}_{36} = \gamma\bar{\boldsymbol{S}}_1\boldsymbol{A}_{d2}^{\boldsymbol{T}}$, $\bar{\boldsymbol{\Theta}}_{37} = \alpha\bar{\boldsymbol{S}}_1\boldsymbol{A}_{d2}^{\mathrm{T}}$, $\bar{\boldsymbol{\Theta}}_{44} = -(\bar{\boldsymbol{Q}}_{\boldsymbol{h}2} - \bar{\boldsymbol{Q}}_{\boldsymbol{h}4}) - \bar{\boldsymbol{R}}_{\boldsymbol{h}1} + \delta(\bar{\boldsymbol{M}}_{h1} + \bar{\boldsymbol{M}}_{h1}^{\mathrm{T}})$, $\bar{\boldsymbol{\Theta}}_{45} = \lambda\boldsymbol{B}\boldsymbol{V} + \delta(-\bar{\boldsymbol{M}}_{h1} + \bar{\boldsymbol{N}}_{h1}^{\mathrm{T}})$, $\bar{\boldsymbol{\Theta}}_{47} = -\lambda\bar{\boldsymbol{S}}_1^{\mathrm{T}}$, $\bar{\boldsymbol{\Theta}}_{48} = \lambda\boldsymbol{D}$, $\bar{\boldsymbol{\Theta}}_{55} = \beta\boldsymbol{B}\boldsymbol{V} + \beta\boldsymbol{V}^{\mathrm{T}}\boldsymbol{B}^{\mathrm{T}} - \sum_{\boldsymbol{k}=3}^{4}\bar{\boldsymbol{Q}}_{hk} + \delta(-\bar{\boldsymbol{N}}_{h1} - \bar{\boldsymbol{N}}_{h1}^{\mathrm{T}}) + \delta(\bar{\boldsymbol{M}}_{h2} + \bar{\boldsymbol{M}}_{h2}^{\mathrm{T}})$, $\bar{\boldsymbol{\Theta}}_{56} = \gamma\boldsymbol{V}^{\mathrm{T}}\boldsymbol{B}^{\mathrm{T}} + \delta(-\bar{\boldsymbol{M}}_{h2} + \bar{\boldsymbol{N}}_{h2}^{\mathrm{T}})$, $\bar{\boldsymbol{\Theta}}_{57} = -\beta\bar{\boldsymbol{S}}_1^{\mathrm{T}} + \alpha\boldsymbol{V}^{\mathrm{T}}\boldsymbol{B}^{\mathrm{T}}$, $\bar{\boldsymbol{\Theta}}_{58} = \beta\boldsymbol{D}$, $\bar{\boldsymbol{\Theta}}_{66} = -\bar{\boldsymbol{Q}}_{h1} + \delta(-\bar{\boldsymbol{N}}_{h2} - \bar{\boldsymbol{N}}_{h2}^{\mathrm{T}})$, $\bar{\boldsymbol{\Theta}}_{67} = -\gamma\bar{\boldsymbol{S}}_1^{\mathrm{T}}$, $\bar{\boldsymbol{\Theta}}_{68} = \gamma\boldsymbol{D}$, $\bar{\boldsymbol{\Theta}}_{77} = -\alpha\bar{\boldsymbol{S}}_1^{\mathrm{T}} - \alpha\bar{\boldsymbol{S}}_1 + \bar{\boldsymbol{R}}_h + \bar{\boldsymbol{R}}_\tau$, $\bar{\boldsymbol{\Theta}}_{78} = \alpha\boldsymbol{D}$, $\bar{\boldsymbol{\Theta}}_{88} = -\Gamma^2\boldsymbol{I}$, $\bar{\boldsymbol{\Theta}}_{99} = -\boldsymbol{I}$, $\boldsymbol{K} = \boldsymbol{Y}(\bar{\boldsymbol{S}}_1^{\mathrm{T}})^{-1}$, $\boldsymbol{K}_{\boldsymbol{h}} = \boldsymbol{V}(\bar{\boldsymbol{S}}_1^{\mathrm{T}})^{-1}$, $\bar{\boldsymbol{R}}_h = h_{(i-1)}^2\bar{\boldsymbol{R}}_{h1} + \delta^2\bar{\boldsymbol{R}}_{h2}$, $\bar{\boldsymbol{R}}_\tau = \tau_1^2\bar{\boldsymbol{R}}_{\tau_1} + \tau_1^2\bar{\boldsymbol{R}}_{\tau_2}$.

Proof: considering the i^{th} instance when $h \in [h_{(i-1)}, h_i]$, a simple LK function is defined as [34]:

$$V_i(t)=V_1(t)+V_{i2}(t) \tag{28}$$

$$V_1(t)=\boldsymbol{x}^{\mathrm{T}}(t)\boldsymbol{P}\boldsymbol{x}(t)+\sum_{i=1}^{2}\int_{t-\tau_i}^{t}\boldsymbol{x}^{\mathrm{T}}(s)\boldsymbol{Q}_i\boldsymbol{x}(s)\mathrm{d}s+\sum_{i=1}^{2}\tau_i\int_{t-\tau_i}^{t}\int_{\theta}^{t}\dot{\boldsymbol{x}}^{\mathrm{T}}(\phi)\boldsymbol{R}_{\tau i}\dot{\boldsymbol{x}}(\phi)\mathrm{d}\phi\mathrm{d}\theta \tag{29}$$

$$\begin{aligned}V_{i2}(t)=&\sum_{j=1}^{2}\int_{t-h_{i+1-j}}^{t}\boldsymbol{x}^{\mathrm{T}}(\theta)\boldsymbol{Q}_{hj}x(\theta)\mathrm{d}\theta+\\&\int_{t-h}^{t}\boldsymbol{x}^{\mathrm{T}}(\theta)\boldsymbol{Q}_{h3}x(\theta)\mathrm{d}\theta+\int_{t-h}^{t-h_{i-1}}x^{\mathrm{T}}(\theta)\boldsymbol{Q}_{h4}x(\theta)\mathrm{d}\theta+\\&h_{(i-1)}\int_{t-h_{i-1}}^{t}\int_{\theta}^{t}\dot{\boldsymbol{x}}^{\mathrm{T}}(\phi)\boldsymbol{R}_{h1}\dot{\boldsymbol{x}}(\phi)\mathrm{d}\phi\mathrm{d}\theta+\\&\delta\int_{t-h_i}^{t-h_{i-1}}\int_{\theta}^{t}\dot{\boldsymbol{x}}^{\mathrm{T}}(\phi)\boldsymbol{R}_{h2}\dot{\boldsymbol{x}}(\phi)\mathrm{d}\phi\mathrm{d}\theta\end{aligned} \tag{30}$$

Differentiating $V_i(t)$ with respect to time along the state trajectory of (23) yields:

$$\dot{V}_i(t)=\dot{V}_1(t)+\dot{V}_{i2}(t) \tag{31}$$

$$\begin{aligned}\dot{V}_1(t)=&2\boldsymbol{x}^{\mathrm{T}}(t)\boldsymbol{P}\dot{\boldsymbol{x}}(t)+\sum_{k=1}^{2}\boldsymbol{x}^{\mathrm{T}}(t)\boldsymbol{Q}_k\boldsymbol{x}(t)-\\&\sum_{i=1}^{2}\boldsymbol{x}^{\mathrm{T}}(t-\tau_i)\boldsymbol{Q}_i x(t-\tau_i)+\dot{\boldsymbol{x}}^{\mathrm{T}}(t)\boldsymbol{R}_\tau\dot{\boldsymbol{x}}(t)-\\&\sum_{i=1}^{2}\tau_i\int_{t-\tau_i}^{t}\dot{\boldsymbol{x}}^{\mathrm{T}}(\theta)\boldsymbol{R}_{\tau i}\dot{\boldsymbol{x}}(\theta)\mathrm{d}\theta\end{aligned} \tag{32}$$

$$\begin{aligned}\dot{V}_{i2}(t)=&\sum_{k=1}^{3}\boldsymbol{x}^{\mathrm{T}}(t)\boldsymbol{Q}_{hk}\boldsymbol{x}(t)-\boldsymbol{x}^{\mathrm{T}}(t-h_{i-1})(\boldsymbol{Q}_{h2}-\boldsymbol{Q}_{h4})\boldsymbol{x}(t-h_{i-1})-\\&\boldsymbol{x}^{\mathrm{T}}(t-h_i)\boldsymbol{Q}_{h1}\boldsymbol{x}(t-h_i)-\sum_{k=3}^{4}\boldsymbol{x}^{\mathrm{T}}(t-h)\boldsymbol{Q}_{hk}\boldsymbol{x}(t-h)+\\&\dot{\boldsymbol{x}}^{\mathrm{T}}(t)\boldsymbol{R}_h\dot{\boldsymbol{x}}(t)-h_{i-1}\int_{t-h_{i-1}}^{t}\dot{\boldsymbol{x}}^{\mathrm{T}}(\theta)\boldsymbol{R}_{h1}\dot{\boldsymbol{x}}(\theta)\mathrm{d}\theta-\\&\delta\int_{t-h_i}^{t-h_{i-1}}\dot{\boldsymbol{x}}^{\mathrm{T}}(\theta)\boldsymbol{R}_{h2}\dot{\boldsymbol{x}}(\theta)\mathrm{d}\theta\end{aligned} \tag{33}$$

where $\boldsymbol{R}_\tau=\tau_1^2\boldsymbol{R}_{\tau_1}+\tau_2^2\boldsymbol{R}_{\tau_2}$ and $\boldsymbol{R}_h=h_{i-1}^2\boldsymbol{R}_{h1}+\delta^2\boldsymbol{R}_{h2}$.

Instead of replacing $\dot{\boldsymbol{x}}(t)$ by directly using (23) in (31), we consider in this paper a zero valued quadratic formulation of the system dynamics (23) as:

$$\begin{aligned}&\big(2\boldsymbol{x}^{\mathrm{T}}(t)\boldsymbol{S}_1+2\boldsymbol{x}^{\mathrm{T}}(t-h_{i-1})\boldsymbol{S}_2+2\boldsymbol{x}^{\mathrm{T}}(t-h)\boldsymbol{S}_3+2\boldsymbol{x}^{\mathrm{T}}(t-h_i)\boldsymbol{S}_4+\\&2\dot{\boldsymbol{x}}^{\mathrm{T}}(t)\boldsymbol{S}_5\big)\times\big(-\dot{\boldsymbol{x}}(t)+\boldsymbol{A}_c\boldsymbol{x}(t)+\boldsymbol{B}_h\boldsymbol{x}(t-h)+\boldsymbol{A}_{d1}\boldsymbol{x}(t-\tau_1)+\\&\boldsymbol{A}_{d2}\boldsymbol{x}(t-\tau_2)+\boldsymbol{D}\boldsymbol{w}(t)\big)=0\end{aligned} \tag{34}$$

where $\boldsymbol{S}_k$, $k=1,2,\dots,5$ are arbitrary matrices of appropriate dimensions. This will incorporate the information regarding the coupling of some important states with the system dynamics. As $\dot{\boldsymbol{x}}(t)$ is not replaced from (23) to (31), it is an important requirement for the analysis to incorporate the information regarding the system dynamics. Therefore, the above zero term (34) can be used in the analysis. This term can easily fulfill the requirement of involving states of system dynamics coupled with some important states while modifying the stabilization requirement. The following inequality is used [35] to separate the cross-product term in (34).

$$2\boldsymbol{\xi}^{\mathrm{T}}(t)\boldsymbol{S}\boldsymbol{w}(t)\le\Gamma^{-2}\boldsymbol{\xi}^{\mathrm{T}}(t)\boldsymbol{S}\boldsymbol{S}^{\mathrm{T}}\boldsymbol{\xi}(t)+\Gamma^2\boldsymbol{w}^{\mathrm{T}}(t)\boldsymbol{w}(t) \tag{35}$$

where $\boldsymbol{S}=\left[\boldsymbol{D}^{\mathrm{T}}\boldsymbol{S}_1^{\mathrm{T}},\boldsymbol{0},\boldsymbol{0},\boldsymbol{D}^{\mathrm{T}}\boldsymbol{S}_2^{\mathrm{T}},\boldsymbol{D}^{\mathrm{T}}\boldsymbol{S}_3^{\mathrm{T}},\boldsymbol{D}^{\mathrm{T}}\boldsymbol{S}_4^{\mathrm{T}},\boldsymbol{D}^{\mathrm{T}}\boldsymbol{S}_5^{\mathrm{T}}\right]^{\mathrm{T}}$, and $\boldsymbol{\xi}(t)=\left[\boldsymbol{x}^{\mathrm{T}}(t),\boldsymbol{x}^{\mathrm{T}}(t-\tau_1),\boldsymbol{x}^{\mathrm{T}}(t-\tau_2),\boldsymbol{x}^{\mathrm{T}}(t-h_{i-1}),\boldsymbol{x}^{\mathrm{T}}(t-h),\boldsymbol{x}^{\mathrm{T}}(t-h_i),\dot{\boldsymbol{x}}^{\mathrm{T}}(t)\right]^{\mathrm{T}}$.

Following (25) of Lemma 1, two integral terms of $\dot{V}_1(t)$ and the first integral of $\dot{V}_{i2}(t)$ are approximated. The last integral term of $\dot{V}_{i2}(t)$ in (31) may be written as:

$$\begin{aligned}-\delta\int_{t-h_i}^{t-h_{i-1}}\dot{\boldsymbol{x}}^{\mathrm{T}}(\theta)\boldsymbol{R}_{h2}\dot{\boldsymbol{x}}(\theta)\mathrm{d}\theta=&-\delta\int_{t-h}^{t-h_{i-1}}\dot{\boldsymbol{x}}^{\mathrm{T}}(\theta)\boldsymbol{R}_{h2}\dot{\boldsymbol{x}}(\theta)\mathrm{d}\theta-\\&\delta\int_{t-h_i}^{t-h}\dot{\boldsymbol{x}}^{\mathrm{T}}(\theta)\boldsymbol{R}_{h2}\dot{\boldsymbol{x}}(\theta)\mathrm{d}\theta\end{aligned} \tag{36}$$

The above term (36) can be approximated by following (26) of Lemma 1. After the approximation of all integral terms in (31), we can write the stability condition as:

$$\begin{aligned}\dot{V}_i(x_t,\dot{x}_t)\le\boldsymbol{\xi}^{\mathrm{T}}(t)\Big[\overline{\Psi}+h_{i-1}^2\Omega_i+\rho\delta^2\boldsymbol{\Phi}_1\boldsymbol{R}_{h2}^{-1}\boldsymbol{\Phi}_1^{\mathrm{T}}+\\(1-\rho)\delta^2\boldsymbol{\Phi}_2\boldsymbol{R}_{h2}^{-1}\boldsymbol{\Phi}_2^{\mathrm{T}}\Big]\xi(t)\end{aligned} \tag{37}$$

where $\bar{\boldsymbol{\Psi}}=\boldsymbol{\Psi}+\hat{\boldsymbol{\Psi}}$, $\hat{\boldsymbol{\Psi}}=\Gamma^{-2}\xi^{\mathrm{T}}(t)\boldsymbol{S}\boldsymbol{S}^{\mathrm{T}}\xi(t)+\Gamma^2\boldsymbol{w}^{\mathrm{T}}(t)\boldsymbol{w}(t)$, $\boldsymbol{\Psi}=[\boldsymbol{\Psi}_{ij}]_{i,j=1,2,\dots,7}$, $\boldsymbol{\Psi}_{11}=\boldsymbol{S}_1\boldsymbol{A}_c+\boldsymbol{A}_c^{\mathrm{T}}\boldsymbol{S}_1^{\mathrm{T}}+\sum_{k=1}^{2}\boldsymbol{Q}_k-\boldsymbol{R}_{h1}-\boldsymbol{R}_{\tau_1}-\boldsymbol{R}_{\tau_2}+\sum_{k=1}^{3}\boldsymbol{Q}_{hk}$, $\boldsymbol{\Psi}_{12}=\boldsymbol{S}_1\boldsymbol{A}_{d1}+\boldsymbol{R}_{\tau_1}$, $\boldsymbol{\Psi}_{13}=\boldsymbol{S}_1\boldsymbol{A}_{d2}+\boldsymbol{R}_{\tau_2}$, $\boldsymbol{\Psi}_{14}=\boldsymbol{A}_c^{\mathrm{T}}\boldsymbol{S}_2^{\mathrm{T}}+\boldsymbol{R}_{h1}$, $\boldsymbol{\Psi}_{15}=\boldsymbol{A}_c^{\mathrm{T}}\boldsymbol{S}_3^{\mathrm{T}}+\boldsymbol{S}_1\boldsymbol{B}_h$, $\boldsymbol{\Psi}_{16}=\boldsymbol{A}_c^{\mathrm{T}}\boldsymbol{S}_4^{\mathrm{T}}$, $\boldsymbol{\Psi}_{17}=-\boldsymbol{S}_1+\boldsymbol{A}_c^{\mathrm{T}}\boldsymbol{S}_5^{\mathrm{T}}+\boldsymbol{P}$, $\boldsymbol{\Psi}_{22}=-\boldsymbol{Q}_1-\boldsymbol{R}_{\tau_1}$, $\boldsymbol{\Psi}_{24}=\boldsymbol{A}_{d1}^{\mathrm{T}}\boldsymbol{S}_2^{\mathrm{T}}$, $\boldsymbol{\Psi}_{25}=\boldsymbol{A}_{d1}^{\mathrm{T}}\boldsymbol{S}_3^{\mathrm{T}}$, $\boldsymbol{\Psi}_{26}=\boldsymbol{A}_{d1}^{\mathrm{T}}\boldsymbol{S}_4^{\mathrm{T}}$, $\boldsymbol{\Psi}_{27}=\boldsymbol{A}_{d1}^{\mathrm{T}}\boldsymbol{S}_5^{\mathrm{T}}$, $\boldsymbol{\Psi}_{33}=-\boldsymbol{Q}_2-\boldsymbol{R}_{\tau_2}$, $\boldsymbol{\Psi}_{34}=\boldsymbol{A}_{d2}^{\mathrm{T}}\boldsymbol{S}_2^{\mathrm{T}}$, $\boldsymbol{\Psi}_{35}=\boldsymbol{A}_{d2}^{\mathrm{T}}\boldsymbol{S}_3^{\mathrm{T}}$, $\boldsymbol{\Psi}_{36}=\boldsymbol{A}_{d2}^{\mathrm{T}}\boldsymbol{S}_4^{\mathrm{T}}$, $\boldsymbol{\Psi}_{37}=\boldsymbol{A}_{d2}^{\mathrm{T}}\boldsymbol{S}_5^{\mathrm{T}}$, $\boldsymbol{\Psi}_{44}=-(\boldsymbol{Q}_{h2}-\boldsymbol{Q}_{h4})-\boldsymbol{R}_{h1}+\delta(\boldsymbol{M}_{h1}+\boldsymbol{M}_{h1}^{\mathrm{T}})$, $\boldsymbol{\Psi}_{45}=\boldsymbol{S}_2\boldsymbol{B}_h+\delta(-\boldsymbol{M}_{h1}+\boldsymbol{N}_{h1}^{\mathrm{T}})$, $\boldsymbol{\Psi}_{47}=-\boldsymbol{S}_2$, $\boldsymbol{\Psi}_{55}=\boldsymbol{S}_3\boldsymbol{B}_h+\boldsymbol{B}_h^{\mathrm{T}}\boldsymbol{S}_3^{\mathrm{T}}-\sum_{k=3}^{4}\boldsymbol{Q}_{hk}+\delta(-\boldsymbol{N}_{h1}-\boldsymbol{N}_{h1}^{\mathrm{T}})+\delta(\boldsymbol{M}_{h2}+\boldsymbol{M}_{h2}^{\mathrm{T}})$, $\boldsymbol{\Psi}_{56}=\boldsymbol{B}_h^{\mathrm{T}}\boldsymbol{S}_4^{\mathrm{T}}+\delta(-\boldsymbol{M}_{h2}+\boldsymbol{N}_{h2}^{\mathrm{T}})$, $\boldsymbol{\Psi}_{57}=-\boldsymbol{S}_3+\boldsymbol{B}_h^{\mathrm{T}}\boldsymbol{S}_5^{\mathrm{T}}$, $\boldsymbol{\Psi}_{66}=-\boldsymbol{Q}_{h1}+\delta(-\boldsymbol{N}_{h2}-\boldsymbol{N}_{h2}^{\mathrm{T}})$, $\boldsymbol{\Psi}_{67}=-\boldsymbol{S}_4$, $\boldsymbol{\Psi}_{77}=-\boldsymbol{S}_5-\boldsymbol{S}_5^{\mathrm{T}}+\delta^2\boldsymbol{R}_{h2}+(\tau_1^2\boldsymbol{R}_{\tau_1}+\tau_2^2\boldsymbol{R}_{\tau_1})$, $\rho=\dfrac{h-h_{i-1}}{\delta}\ (0\le\rho\le1)$, $\Omega_i=\begin{bmatrix}\boldsymbol{0}_{6n\times 6n} & \boldsymbol{0}_{6n\times n}\\ \boldsymbol{0}_{n\times 6n} & \boldsymbol{R}_{h1}\end{bmatrix}$, $\boldsymbol{\Phi}_1=\left[\boldsymbol{0}\ \ \boldsymbol{0}\ \ \boldsymbol{0}\ \ \boldsymbol{M}_{h1}^{\mathrm{T}}\ \ \boldsymbol{N}_{h1}^{\mathrm{T}}\ \ \boldsymbol{0}\ \ \boldsymbol{0}\right]^{\mathrm{T}}$, and $\boldsymbol{\Phi}_2=\left[\boldsymbol{0}\ \ \boldsymbol{0}\ \ \boldsymbol{0}\ \ \boldsymbol{M}_{h2}^{\mathrm{T}}\ \ \boldsymbol{N}_{h2}^{\mathrm{T}}\ \ \boldsymbol{0}\ \ \boldsymbol{0}\right]^{\mathrm{T}}$.

Therefore, the stability requirement of the i^{th} interval is:

$$\overline{\Psi}+h_{i-1}^2\Omega_i+\rho\delta^2\boldsymbol{\Phi}_1\boldsymbol{R}_{h2}^{-1}\boldsymbol{\Phi}_1^{\mathrm{T}}+(1-\rho)\delta^2\boldsymbol{\Phi}_2\boldsymbol{R}_{h2}^{-1}\boldsymbol{\Phi}_2^{\mathrm{T}}<0 \tag{38}$$

Next, to ascertain the H_∞ performance criterion, the performance criterion from (2) can be obtained as:

$$J_{yw}=\int_0^\infty\left(\boldsymbol{y}^{\mathrm{T}}(t)\boldsymbol{y}(t)-\Gamma^2\boldsymbol{w}^{\mathrm{T}}(t)\boldsymbol{w}(t)\right)\mathrm{d}t \tag{39}$$

Note that if $J_{yw}\le0$, the system (23) satisfies the condition (2). Thus, to design an H_∞ performance based two-term controller with Γ performance index, the H_∞ performance criterion $J_{yw}\le0$ is adopted. For zero initial condition, i.e., $V(0)=0$, and since $V(\infty)\ge0$, (39) can be re-written as:

$$J_{yw}\le\int_0^\infty\left(\boldsymbol{y}^{\mathrm{T}}(t)\boldsymbol{y}(t)-\Gamma^2\boldsymbol{w}^{\mathrm{T}}(t)\boldsymbol{w}(t)+\dot{V}_i(t)\right)\mathrm{d}t \tag{40}$$

Substituting (38) into (40), the following inequality can be obtained:

$$J_{yw}\le\int_0^\infty\boldsymbol{\xi}^{\mathrm{T}}(t)\boldsymbol{\Xi}\boldsymbol{\xi}(t)\mathrm{d}t \tag{41}$$

where $\boldsymbol{\Xi}=\Psi+h_{i-1}^2\Omega_i+\bar{\boldsymbol{C}}\bar{\boldsymbol{C}}^{\mathrm{T}}+\rho\delta^2\boldsymbol{\Phi}_1\boldsymbol{R}_{h2}^{-1}\boldsymbol{\Phi}_1^{\mathrm{T}}+\left(1-\rho\right)\delta^2\boldsymbol{\Phi}_2\boldsymbol{R}_{h2}^{-1}\boldsymbol{\Phi}_2^{\mathrm{T}}$, and $\bar{\boldsymbol{C}}=\left[\boldsymbol{C}\ \ 0\ \ 0\ \ 0\ \ 0\ \ 0\ \ 0\right]^{\mathrm{T}}$.

Therefore, $J_{yw}\le0$ is satisfied if $\boldsymbol{\Xi}<\boldsymbol{0}$. The above is a polytope of matrices on ρ, and it is always negative definite if two of its vertices are also negative definite. Then, (38) can be equivalently written as:

$$\Psi + h_{i-1}^2 \Omega_i + \bar{\boldsymbol{C}}\bar{\boldsymbol{C}}^{\mathrm{T}} + \delta^2 \boldsymbol{\Phi}_j \boldsymbol{R}_{h2}^{-1} \boldsymbol{\Phi}_j^{\mathrm{T}} < 0 \quad j = 1, 2 \tag{42}$$

Note that $\Omega_i \geq 0$ and it is maximum in the N^{th} interval where $h \in [h_{N-1}, \bar{h}]$. Therefore, irrespective of h lies in any of the intervals, the following condition always ensures stability of (23):

$$\Psi + h_{N-1}^2 \Omega_N + \bar{\boldsymbol{C}}\bar{\boldsymbol{C}}^{\mathrm{T}} + \delta^2 \boldsymbol{\Phi}_j \boldsymbol{R}_{h2}^{-1} \boldsymbol{\Phi}_j^{\mathrm{T}} < 0 \quad j = 1, 2 \tag{43}$$

Taking Schur complement for the last term in (43), we can obtain:

$$\begin{bmatrix} \boldsymbol{\Theta} & \delta \boldsymbol{\Phi}_j \\ (\delta \boldsymbol{\Phi}_j)^{\mathrm{T}} & -\boldsymbol{R}_{h2} \end{bmatrix} < \boldsymbol{0} \quad j = 1, 2 \tag{44}$$

where $\boldsymbol{\Theta}_{11} = \boldsymbol{\Psi}_{11}$, $\boldsymbol{\Theta}_{12} = \boldsymbol{\Psi}_{12}$, $\boldsymbol{\Theta}_{13} = \boldsymbol{\Psi}_{13}$, $\boldsymbol{\Theta}_{14} = \boldsymbol{\Psi}_{14}$, $\boldsymbol{\Theta}_{15} = \boldsymbol{\Psi}_{15}$, $\boldsymbol{\Theta}_{16} = \boldsymbol{\Psi}_{16}$, $\boldsymbol{\Theta}_{17} = \boldsymbol{\Psi}_{17}$, $\boldsymbol{\Theta}_{18} = \boldsymbol{S}_1 \boldsymbol{D}$, $\boldsymbol{\Theta}_{19} = \boldsymbol{C}^{\mathrm{T}}$, $\boldsymbol{\Theta}_{22} = \boldsymbol{\Psi}_{22}$, $\boldsymbol{\Theta}_{23} = \boldsymbol{\Psi}_{23}$, $\boldsymbol{\Theta}_{24} = \boldsymbol{\Psi}_{24}$, $\boldsymbol{\Theta}_{25} = \boldsymbol{\Psi}_{25}$, $\boldsymbol{\Theta}_{26} = \boldsymbol{\Psi}_{26}$, $\boldsymbol{\Theta}_{27} = \boldsymbol{\Psi}_{27}$, $\boldsymbol{\Theta}_{28} = \boldsymbol{0}$, $\boldsymbol{\Theta}_{29} = \boldsymbol{0}$, $\boldsymbol{\Theta}_{33} = \boldsymbol{\Psi}_{33}$, $\boldsymbol{\Theta}_{34} = \boldsymbol{\Psi}_{34}$, $\boldsymbol{\Theta}_{35} = \boldsymbol{\Psi}_{35}$, $\boldsymbol{\Theta}_{36} = \boldsymbol{\Psi}_{36}$, $\boldsymbol{\Theta}_{37} = \boldsymbol{\Psi}_{37}$, $\boldsymbol{\Theta}_{38} = \boldsymbol{0}$, $\boldsymbol{\Theta}_{39} = \boldsymbol{0}$, $\boldsymbol{\Theta}_{44} = \boldsymbol{\Psi}_{44}$, $\boldsymbol{\Theta}_{45} = \boldsymbol{\Psi}_{45}$, $\boldsymbol{\Theta}_{46} = \boldsymbol{\Psi}_{46}$, $\boldsymbol{\Theta}_{47} = \boldsymbol{\Psi}_{47}$, $\boldsymbol{\Theta}_{48} = \boldsymbol{S}_2 \boldsymbol{D}$, $\boldsymbol{\Theta}_{49} = \boldsymbol{0}$, $\boldsymbol{\Theta}_{55} = \boldsymbol{\Psi}_{55}$, $\boldsymbol{\Theta}_{56} = \boldsymbol{\Psi}_{56}$, $\boldsymbol{\Theta}_{57} = \boldsymbol{\Psi}_{57}$, $\boldsymbol{\Theta}_{58} = \boldsymbol{S}_3 \boldsymbol{D}$, $\boldsymbol{\Theta}_{59} = \boldsymbol{0}$, $\boldsymbol{\Theta}_{66} = \boldsymbol{\Psi}_{66}$, $\boldsymbol{\Theta}_{67} = \boldsymbol{\Psi}_{67}$, $\boldsymbol{\Theta}_{68} = \boldsymbol{S}_4 \boldsymbol{D}$, $\boldsymbol{\Theta}_{69} = \boldsymbol{0}$, $\boldsymbol{\Theta}_{77} = \boldsymbol{\Psi}_{77} + \boldsymbol{h}_{(N-1)}^2 \boldsymbol{R}_{h1}$, $\boldsymbol{\Theta}_{78} = \boldsymbol{S}_5 \boldsymbol{D}$, $\boldsymbol{\Theta}_{79} = \boldsymbol{0}$, $\boldsymbol{\Theta}_{88} = -\Gamma^2 \boldsymbol{I}$, $\boldsymbol{\Theta}_{89} = \boldsymbol{0}$, and $\boldsymbol{\Theta}_{99} = -\boldsymbol{I}$.

The derived inequality (44) is not an LMI because it has some nonlinear terms in $\boldsymbol{\Theta}$. The presence of five arbitrary matrices $\boldsymbol{S}_1$, $\boldsymbol{S}_2$, $\boldsymbol{S}_3$, $\boldsymbol{S}_4$ and $\boldsymbol{S}_5$ in $\boldsymbol{\Theta}$ makes the inequality (44) nonlinear. Thus, the inequality (44) can be converted into LMI by restricting the presence of five arbitrary matrices into only one arbitrary matrix (i.e., $\boldsymbol{S}_1$). For this reason, four parameters such as λ, β, γ and α are chosen by the control designer. $\boldsymbol{S}_2$, $\boldsymbol{S}_3$, $\boldsymbol{S}_4$ and $\boldsymbol{S}_5$ can be represented in terms of $\boldsymbol{S}_1$ by using λ, β, γ, and α as $\boldsymbol{S}_2 = \lambda \boldsymbol{S}_1$, $\boldsymbol{S}_3 = \beta \boldsymbol{S}_1$, $\boldsymbol{S}_4 = \gamma \boldsymbol{S}_1$, and $\boldsymbol{S}_5 = \alpha \boldsymbol{S}_1$, respectively.

The LMI (27) can be obtained by substituting $\boldsymbol{S}_2 = \lambda \boldsymbol{S}_1$, $\boldsymbol{S}_3 = \beta \boldsymbol{S}_1$, $\boldsymbol{S}_4 = \gamma \boldsymbol{S}_1$, and $\boldsymbol{S}_5 = \alpha \boldsymbol{S}_1$ into (44), pre- and post-multiplying (44) by $diag\{\boldsymbol{S}_1^{-1}\ \boldsymbol{S}_1^{-1}\ \boldsymbol{S}_1^{-1}\ \boldsymbol{S}_1^{-1}\ \boldsymbol{S}_1^{-1}\ \boldsymbol{S}_1^{-1}\ \boldsymbol{S}_1^{-1}\ \boldsymbol{I}\ \boldsymbol{I}\ \boldsymbol{S}_1^{-1}\}$ and its transpose, respectively. Finally, we can change the following variables: $\bar{\boldsymbol{S}}_1 = \boldsymbol{S}_1^{-1}$, $\bar{\boldsymbol{P}} = \bar{\boldsymbol{S}}_1 \boldsymbol{P} \bar{\boldsymbol{S}}_1^{\mathrm{T}}$, $\bar{\boldsymbol{M}}_{hi} = \bar{\boldsymbol{S}}_1 \boldsymbol{M}_{hi} \bar{\boldsymbol{S}}_1^{\mathrm{T}}$, $\bar{\boldsymbol{N}}_{hi} = \bar{\boldsymbol{S}}_1 \boldsymbol{N}_{hi} \bar{\boldsymbol{S}}_1^{\mathrm{T}}$, $\bar{\boldsymbol{Q}}_i = \bar{\boldsymbol{S}}_1 \boldsymbol{Q}_i \bar{\boldsymbol{S}}_1^{\mathrm{T}}$ ($i = 1, 2$), $\bar{\boldsymbol{Q}}_{\boldsymbol{hj}} = \bar{\boldsymbol{S}}_1 \boldsymbol{Q}_{hj} \bar{\boldsymbol{S}}_1^{\mathrm{T}}$ ($j = 1, 2, \ldots, 4$), $\boldsymbol{Y} = \boldsymbol{K} \bar{\boldsymbol{S}}_1^{\mathrm{T}}$, and $\boldsymbol{V} = \boldsymbol{K}_h \bar{\boldsymbol{S}}_1^{\mathrm{T}}$. The proof is completed.

The controller gains can be obtained by using $\boldsymbol{K} = \boldsymbol{Y}(\bar{\boldsymbol{S}}_1^{\mathrm{T}})^{-1}$ and $\boldsymbol{K}_h = \boldsymbol{V}(\bar{\boldsymbol{S}}_1^{\mathrm{T}})^{-1}$ from the feasible solution of (27) with a suitable value of Γ. To obtain the suitable value of Γ, we have to optimize Γ^2 in (27). Thus, an optimal controller is yielded by defining $\Gamma^2 = \bar{\Gamma}$ and minimizing $\bar{\Gamma}$ to obtain a solution of (27). The optimal controller gives optimized value of Γ, but provides high value of controller gains. These high controller gains are not practically implementable [10], [36]. Note that the LMI variables $\boldsymbol{Y}$, $\boldsymbol{V}$, and $\bar{\boldsymbol{S}}_1$ are involved in the computation of controller gains $\boldsymbol{K}$ and $\boldsymbol{K}_h$. Hence, to keep the controller gains within the practical limit, the norm of matrices $\|\boldsymbol{Y}\|$, $\|\boldsymbol{V}\|$, and $\|\bar{\boldsymbol{S}}_1^{-1}\|$ should be minimized. We aim to design such an optimal controller, which gives the minimum value of Γ as well as practically implementable values of $\boldsymbol{K}$ and $\boldsymbol{K}_h$. Therefore, an optimization problem can be defined by formulating a multi-objective function, whose objective is to provide suitable values of Γ, $\boldsymbol{K}$ and $\boldsymbol{K}_h$ simultaneously, with LMI constraints as follows [36], [37]:

$$\begin{cases} \min(\bar{\Gamma} + \boldsymbol{y} + \boldsymbol{v} + \boldsymbol{s}) \\ \text{s.t. } (27) \\ \quad \begin{bmatrix} \boldsymbol{yI} & \boldsymbol{Y} \\ \boldsymbol{Y}^{\mathrm{T}} & \boldsymbol{I} \end{bmatrix} > \boldsymbol{0} \\ \quad \begin{bmatrix} \boldsymbol{vI} & \boldsymbol{V} \\ \boldsymbol{V}^{\mathrm{T}} & \boldsymbol{I} \end{bmatrix} > \boldsymbol{0} \\ \quad \begin{bmatrix} \bar{\boldsymbol{S}}_1 & \boldsymbol{I} \\ \boldsymbol{I}^{\mathrm{T}} & \boldsymbol{sI} \end{bmatrix} > \boldsymbol{0} \end{cases} \tag{45}$$

where $\boldsymbol{y}$, $\boldsymbol{v}$, and $\boldsymbol{s}$ are the norms of the matrices $\|\boldsymbol{Y}\|$, $\|\boldsymbol{V}\|$, and $\|\bar{\boldsymbol{S}}_1^{-1}\|$, respectively. By minimizing the above objective function (45), the H_∞ performance (2) can be achieved. The stabilizing controller gains can also be obtained from the minimization. The number of decision variables and size of the LMI in Theorem 1 does not change with number of division of the delay interval N. This is the most important advantage of the proposed approach. No approximation is used to obtain the stability condition (43) from (42). But, the gap in approximating the first integral term of (31) increases with $h_{(i-1)}$, and $h_{(i-1)}$ increases with N. So, the stabilization criterion is indeed ultimately constrained. This limitation arises due to the choice of LK function and the corresponding results may be influenced by the approximations of the first integral term. However, it is easy to search over N to obtain the maximum tolerable $\bar{h}$.

To simplify Theorem 1 by eliminating the number of variables, the following corollary is proposed.

Corollary 1: system (8) with controller (22) for known α, β, λ and γ satisfies the H_∞ performance (2) if there exists $\bar{\boldsymbol{P}} > \boldsymbol{0}$, $\bar{\boldsymbol{Q}}_i > \boldsymbol{0}$, $\bar{\boldsymbol{Q}}_{hk} > \boldsymbol{0}$, $\bar{\boldsymbol{R}}_{\tau i} > \boldsymbol{0}$, $\bar{\boldsymbol{R}}_{hi} > \boldsymbol{0}$ for $k = 1, 2, 3, 4$, and arbitrary matrices $\bar{\boldsymbol{S}}_1$, $\bar{\boldsymbol{M}}_{hi} > \boldsymbol{0}$, $\bar{\boldsymbol{N}}_{hi} > \boldsymbol{0}$, $\boldsymbol{Y}$ and $\boldsymbol{V}$ for $i = 1, 2$, satisfying the following LMI:

$$\begin{bmatrix} \bar{\boldsymbol{\Sigma}} & \delta \bar{\boldsymbol{\Phi}}_j \\ (\delta \bar{\boldsymbol{\Phi}}_j)^{\mathrm{T}} & -\bar{\boldsymbol{R}}_{h2} \end{bmatrix} < \boldsymbol{0} \quad j = 1, 2 \tag{46}$$

where $\bar{\boldsymbol{\Sigma}} = [\bar{\boldsymbol{\Sigma}}_{ij}]_{i,j=1,2,\ldots,9}$, $\bar{\boldsymbol{\Sigma}}_{11} = \bar{\boldsymbol{\Theta}}_{11}$, $\bar{\boldsymbol{\Sigma}}_{12} = \bar{\boldsymbol{\Theta}}_{12}$, $\bar{\boldsymbol{\Sigma}}_{13} = \bar{\boldsymbol{\Theta}}_{13}$, $\bar{\boldsymbol{\Sigma}}_{14} = \bar{\boldsymbol{\Theta}}_{14}$, $\bar{\boldsymbol{\Sigma}}_{15} = \bar{\boldsymbol{\Theta}}_{15}$, $\bar{\boldsymbol{\Sigma}}_{16} = \bar{\boldsymbol{\Theta}}_{16}$, $\bar{\boldsymbol{\Sigma}}_{17} = \bar{\boldsymbol{\Theta}}_{17}$, $\bar{\boldsymbol{\Sigma}}_{18} = \bar{\boldsymbol{\Theta}}_{18}$, $\bar{\boldsymbol{\Sigma}}_{19} = \bar{\boldsymbol{\Theta}}_{19}$, $\bar{\boldsymbol{\Sigma}}_{22} = \bar{\boldsymbol{\Theta}}_{22}$, $\bar{\boldsymbol{\Sigma}}_{24} = \bar{\boldsymbol{\Theta}}_{24}$, $\bar{\boldsymbol{\Sigma}}_{25} = \bar{\boldsymbol{\Theta}}_{25}$, $\bar{\boldsymbol{\Sigma}}_{26} = \bar{\boldsymbol{\Theta}}_{26}$, $\bar{\boldsymbol{\Sigma}}_{27} = \bar{\boldsymbol{\Theta}}_{27}$, $\bar{\boldsymbol{\Sigma}}_{33} = \bar{\boldsymbol{\Theta}}_{33}$, $\bar{\boldsymbol{\Sigma}}_{34} = \bar{\boldsymbol{\Theta}}_{34}$, $\bar{\boldsymbol{\Sigma}}_{35} = \bar{\boldsymbol{\Theta}}_{35}$, $\bar{\boldsymbol{\Sigma}}_{36} = \bar{\boldsymbol{\Theta}}_{36}$, $\bar{\boldsymbol{\Sigma}}_{37} = \bar{\boldsymbol{\Theta}}_{37}$, $\bar{\boldsymbol{\Sigma}}_{44} = -(\bar{\boldsymbol{Q}}_{\boldsymbol{h}2} - \bar{\boldsymbol{Q}}_{\boldsymbol{h}4}) - \bar{\boldsymbol{R}}_{\boldsymbol{h}1} - \bar{\boldsymbol{R}}_{h2}$, $\bar{\boldsymbol{\Sigma}}_{45} = \lambda \boldsymbol{BV} + \bar{\boldsymbol{R}}_{h2}$, $\bar{\boldsymbol{\Sigma}}_{47} = \bar{\boldsymbol{\Theta}}_{47}$, $\bar{\boldsymbol{\Sigma}}_{48} = \bar{\boldsymbol{\Theta}}_{48}$, $\bar{\boldsymbol{\Sigma}}_{55} = \beta \boldsymbol{BV} + \beta \boldsymbol{V}^{\mathrm{T}} \boldsymbol{B}^{\mathrm{T}} - \sum_{k=3}^{4} \bar{\boldsymbol{Q}}_{hk} - 2\bar{\boldsymbol{R}}_{h2}$, $\bar{\boldsymbol{\Sigma}}_{56} = \gamma \boldsymbol{V}^{\mathrm{T}} \boldsymbol{B}^{\mathrm{T}} + \bar{\boldsymbol{R}}_{h2}$, $\bar{\boldsymbol{\Sigma}}_{57} = \bar{\boldsymbol{\Theta}}_{57}$, $\bar{\boldsymbol{\Sigma}}_{58} = \bar{\boldsymbol{\Theta}}_{58}$, $\bar{\boldsymbol{\Sigma}}_{66} = -\bar{\boldsymbol{Q}}_{h1} - \bar{\boldsymbol{R}}_{h2}$, $\bar{\boldsymbol{\Sigma}}_{67} = \bar{\boldsymbol{\Theta}}_{67}$, $\bar{\boldsymbol{\Sigma}}_{68} = \bar{\boldsymbol{\Theta}}_{68}$, $\bar{\boldsymbol{\Sigma}}_{77} = \bar{\boldsymbol{\Theta}}_{77}$, $\bar{\boldsymbol{\Sigma}}_{78} = \bar{\boldsymbol{\Theta}}_{78}$, $\bar{\boldsymbol{\Sigma}}_{88} = \bar{\boldsymbol{\Theta}}_{88}$, and $\bar{\boldsymbol{\Sigma}}_{99} = \bar{\boldsymbol{\Theta}}_{99}$.

Proof: since the last term in (43) is positive definite, one can derive the stability criterion in the form of a single matrix inequality as:

$$\Psi + h_{N-1}^2 \Omega_N + \bar{\boldsymbol{C}}\bar{\boldsymbol{C}}^{\mathrm{T}} + \delta^2 \boldsymbol{\Phi}_1 \boldsymbol{R}_{h2}^{-1} \boldsymbol{\Phi}_1^{\mathrm{T}} + \delta^2 \boldsymbol{\Phi}_2 \boldsymbol{R}_{h2}^{-1} \boldsymbol{\Phi}_2^{\mathrm{T}} < 0 \tag{47}$$

Following Lemma 1, by substituting the free matrix variables as $\boldsymbol{M}_{hi} = \boldsymbol{M}_{hi}^{\mathrm{T}} = -\boldsymbol{N}_{hi} = -\boldsymbol{N}_{hi}^{\mathrm{T}} = -\delta^{-1} \boldsymbol{R}_{h2}$ in (47) and following the linearization technique adopted in Theorem 1, (46) is obtained. The proof is completed.

Although the above stability criterion derived in Corollary 1 is conservative compared to Theorem 1 due to the approximations incorporated, the bounding gap decreases with the decrease of integral limit δ, i.e., the increase of the number of delay intervals (N), in both criteria. Hence, the criterion developed in Corollary 1 is more useful for large N, since it involves less number of free variables. By modifying the single objective problem to a multi-objective one, the gains of the designed controller will be within the practical range. They can be easily implemented in real time.

The proposed Corollary 1 can be used to solve the optimization problem with objective function (45) by replacing the constraint (27) by (46). This causes the reduction of computation complexity with conservative results.

A well-known numerical example is presented below to validate the developed control approach for two-area interconnected power system.

IV. Numerical Example and Result Analysis

An example of a well-known two-area interconnected power system [10] is considered to check the effectiveness of the proposed H_∞ performance based controller design. The parameters of the state space model of the system (3)-(7) is presented in Table I [10], [11].

TABLE I
Parameters of Areas 1 and 2

No.	Parameter	Value of area 1	Value of area 2
1	T_{chi}	0.3 s	0.17 s
2	T_{gi}	0.1 s	0.4 s
3	R_i	0.05	0.05
4	D_i	1	1.5
5	M_i	10	12
6	k_i	0.5	0.5
7	T_{pi}	$M_1/D_1=10$	$M_2/D_2=8$
8	k_{pi}	$1/D_1=1$	$1/D_2=0.667$
9	B_i	$2/R_1+D_1=41$	$2/R_2+D_2=81.5$

For the simulation study of the two-area power system (8) with controller (22) in MATLAB, the delay in the ACE signal of area 1 τ_1 and the delay in the ACE signal of area 2 τ_2 are set to be fixed. To design the controller (22), the gains of the stabilizing controller $\boldsymbol{K}$ and $\boldsymbol{K}_h$ are required. These controller gains with minimized Γ can be obtained from the minimization of objective function (45). The LMI optimization problem containing the objective function (45) can be solved by using *mincx* solver of LMI control Toolbox in MATLAB. However, it is unable to find the solution of the optimization problem using *mincx* solver alone, because *mincx* solver can not get the values of the four parameters λ, β, γ, and α chosen by the control designer as explained in Theorem 1. Now, it is a challenge for the control designer to select suitable values for such unknown parameters, i.e., λ, β, γ, and α. These four unknown parameters can be obtained suitably by using *fminsearch* routine of MATLAB Toolbox. Therefore, the LMI optimization problem is solved by using both *mincx* solver and *fminsearch* routine. The *fminsearch* routine takes four input values at the time of invoking which are treated as initial values for the parameters, then searches the suitable values of λ, β, γ and α, and finally gives the suitable values of these unknown parameters to the *mincx* solver. Then *mincx* solver solves the LMI optimization problem and gives the values of Γ, $\boldsymbol{K}$, $\boldsymbol{K}_h$ along with λ, β, γ and α. Next, the controller (22) is designed by using $\boldsymbol{K}$ and $\boldsymbol{K}_h$.

The maximum tolerable delay margin of the closed loop system (23) can be verified by checking tolerability of delay h_{tol} as well as minimizing Γ. The proposed discretization approach gives an opportunity to study the effect of maximum tolerable delay margin h_{tol} with number of delay intervals N. A study has been made by obtaining h_{tol} using Theorem 1 with respect to change in N and presented in Table II.

TABLE II
Variation of h_{tol} with Respect to Change in N Using Theorem 1

N	h_{tol}	N	h_{tol}	N	h_{tol}
1	0.812	4	0.842	20	0.836
2	0.853	5	0.841	100	0.822
3	0.846	10	0.838	1000	0.821

It can be observed from Table II that the maximum h_{tol} is obtained for $N=2$. However, with the increase in number of delay intervals N, the tolerable delay margin h_{tol} decreases, which is discussed in the previous text. But the reason behind obtaining the maximum tolerability at $N=2$ is that the integral inequalities in (31) are halved, so the bounding gap reduces and leads to improved results. But with the increase of number of delay interval, the tolerable delay margin h_{tol} decreases though the bounding gap in the second integral term decreases. Therefore, one always obtains the maximum tolerable delay margin value at $N=2$.

The major concern in the delay discretization approaches proposed in [28]-[31] is that the number of decision variable increases with the number of delay interval. Therefore, the computation burden increases. But in the proposed approach, the number of decision variable does not increase with the number of delay interval. Therefore, the approach is computationally simple and efficient.

Using the above conditions for simulation, the maximum h_{tol} is also obtained using Corollary 1 by changing the value N. The analysis has been made and presented in Table III. Here, it is also observed that h_{tol} is maximum, i.e., $h_{tol}=0.823$ at $N=2$. But Corollary 1 is conservative than that of the Theorem 1.

TABLE III
Variation h_{tol} with Respect to Change in N Using Corollary 1

N	h_{tol}	N	h_{tol}	N	h_{tol}
1	0.791	4	0.813	20	0.803
2	0.823	5	0.810	100	0.802
3	0.815	10	0.806	1000	0.802

Some variable approximations in Corollary 1 make the criterion conservative. Though the criterion is conservative, the number of variable involved in the criterion is less than that of Theorem 1. From the above study, it is confirmed that the maximum tolerable delay margin h_{tol} can be obtained by setting $N=2$. A comparative analysis is made in Table IV.

TABLE IV
COMPARATIVE ANALYSIS WITH SOME EXISTING RESULTS

Approach	h_{tol}
[10]	0.700
[11]	0.780
Corollary 3	0.823
Theorem 3	0.853

To evaluate the performance of Corollary 1 and Theorem 1 with respect to existing approaches in [10], [11], τ_1 and τ_2 are fixed at 0.1 and 0.2, respectively. The maximum tolerable delay bound h_{tol} obtained using Corollary 1 and Theorem 1 are 0.823 and 0.853, respectively. As compared to the existing approaches in [10], [11], the proposed approach is less conservative with higher value of tolerable delay margin h_{tol}. To validate the approach by simulation, h_{tol} is obtained to be 0.853 by using Theorem 1 at $\alpha=0.5832$, $\beta=0.0179$, $\lambda=0.2675$ and $\gamma=-0.0002$ by minimizing Γ to 9.9912. $\boldsymbol{K}$ and $\boldsymbol{K}_h$ are designed in (48) and (49).

$$\boldsymbol{K}=\begin{bmatrix}-5.0017 & -0.2676 & -0.1273 & 0.0982 & 0.8209 & 0.4753 & 0.0403 & 0.0295 & 0.0260\\ 1.8013 & 0.0801 & 0.0660 & 0.1129 & -3.4306 & -37.4385 & -0.5162 & -1.3949 & -0.3669\end{bmatrix} \tag{48}$$

$$\boldsymbol{K_h}=\begin{bmatrix}-0.4786 & -0.0063 & -0.0199 & -0.0165 & 0.0061 & -0.1240 & -0.0009 & -0.0044 & -0.0022\\ -0.0481 & -0.0017 & -0.0032 & -0.0009 & -0.0734 & -1.3253 & -0.0120 & -0.0523 & -0.0237\end{bmatrix} \tag{49}$$

The deviations in frequency (Δf_1 and Δf_2) and the mechanical power output of the turbines (ΔP_{m1} and ΔP_{m2}) for both the areas modeled in (3)-(7) can be studied with random step load disturbances (ΔP_{d1} and ΔP_{d2}). For simulation, the random step load disturbances of two areas are generated for 200 s as shown in Figs. 4 and 5.

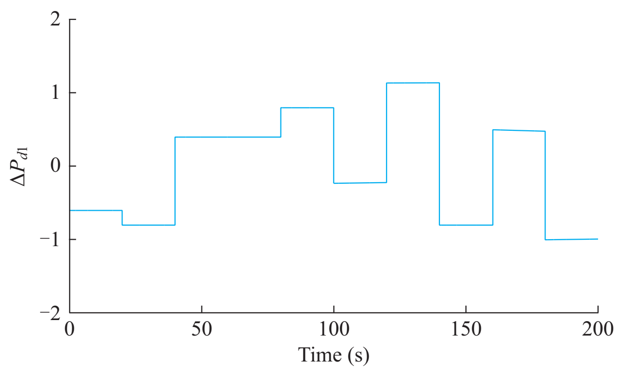

Fig. 4. Change in load disturbance of area 1.

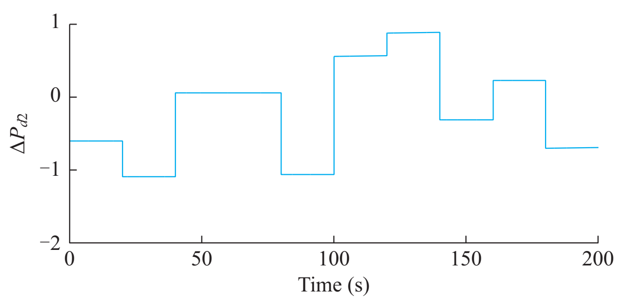

Fig. 5. Change in load disturbance of area 2.

The simulation results Δf_1, Δf_2, ΔP_{m1} and ΔP_{m2} at maximum tolerable delay margin ($h_{tol}=0.853$) are presented in Figs. 6-9, respectively. These results validates that the designed controller ($\boldsymbol{K}$ and $\boldsymbol{K}_h$) is able to achieve stabilization by minimizing the H_∞ performance index Γ to 9.9912 at a tolerable delay margin h_{tol} of 0.853 for random step load disturbances ΔP_{d1} and ΔP_{d2}.

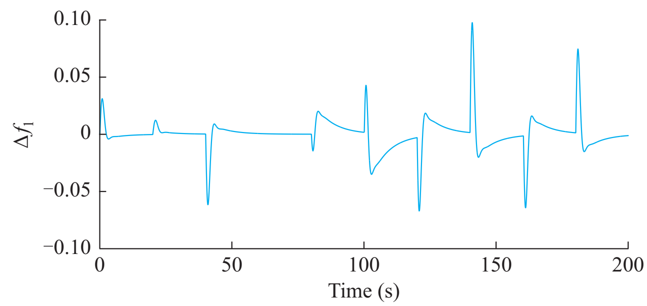

Fig. 6. Change in frequency of area 1.

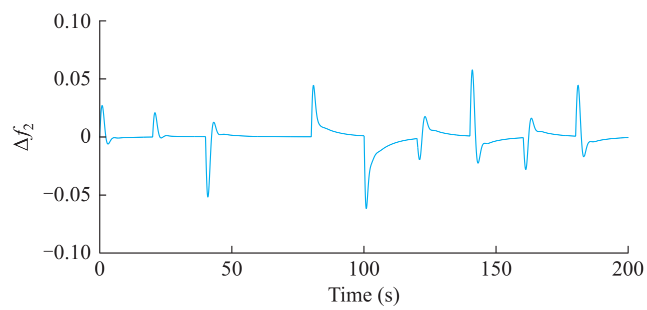

Fig. 7. Change in frequency of area 2.

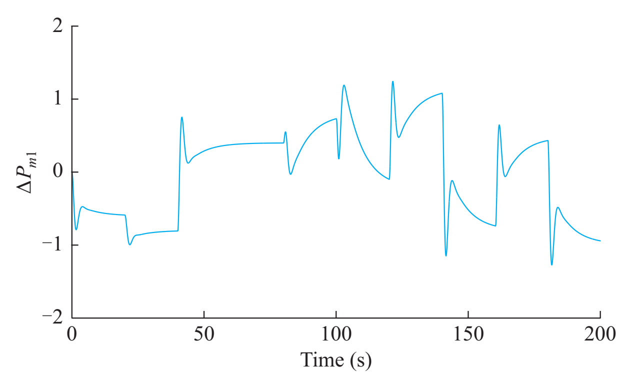

Fig. 8. Deviation in mechanical power output of area 1.

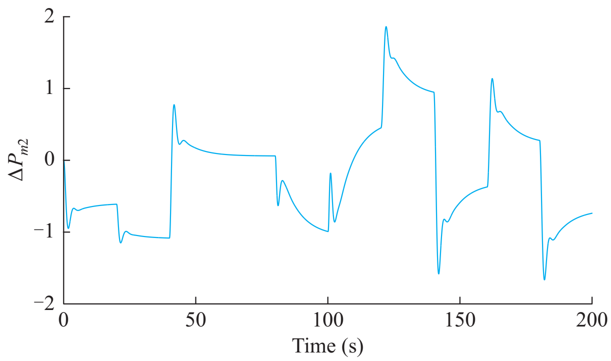

Fig. 9. Deviation in mechanical power output of area 2.

V. Conclusion and Future Scope

In this paper, a delay discretization approach is proposed to improve the tolerable delay margin of the interconnected power system. To validate the approach, a well-known existing example is considered. From the demonstration, it is observed that the designed H_∞ performance based two-term controller is able to withstand random load disturbances. The proposed approach is simple and less conservative than some existing results. Though the approach is simple and less conservative, it is time-consuming and tedious to search the tuning parameters α, β, λ and γ for the minimum Γ. This opens up a new direction for research to avoid the above tuning parameters required during linearization. One may also analyze the tolerable delay margin improvement capability using dynamic state feedback controller in place of a two-term one.

References

[1] M. Ma, C. Zhang, X. Liu *et al.*, "Distributed model predictive load frequency control of the multi-area power system after deregulation," *IEEE Transactions on Industrial Electronics*, vol. 64, no. 6, pp. 5129-5139, Jun. 2017.

[2] Y. Cui, G. Shi, L. Xu *et al.*, "Decentralized H_∞ load frequency control for multi-area power systems with communication uncertainties," in *Advanced Computational Methods in Energy, Power, Electric Vehicles, and Their Integration*, Singapore: Springer, 2017, pp. 429-438.

[3] C. Peng, J. Zhang, H. Yan *et al.*, "Adaptive event-triggering H_∞ load frequency control for network-based power systems," *IEEE Transactions on Industrial Electronics*, vol. 65, no. 2, pp. 1685-1694, Feb. 2018.

[4] C. T. Pan and C. M. Liaw, "An adaptive controller for power system load-frequency control," *IEEE Transactions on Power Systems*, vol. 4, no. 1, pp. 122-128, Feb. 1989.

[5] H. Bevrani and T. Hiyama, "A control strategy for LFC design with communication delays," in *Proceedings of the 7th International Power Engineering Conference*, Singapore, Nov. 2005, pp. 1087-1092.

[6] G. Ray, A. N. Prasad, and G. D. Prasad, "Design of a robust load-frequency controller for interconnected power systems based on the singular-value decomposition method," *Electric Power Systems Research*, vol. 37, no. 3, pp. 209-219, Jun. 1996.

[7] I. P. Kumar and D. P. Kothari, "Recent philosophies of automatic generation control strategies in power systems," *IEEE Transactions on Power Systems*, vol. 20, no. 1, pp. 346-357, Feb. 2005.

[8] L. Jiang, W. Yao, Q. H. Wu *et al.*, "Delay-dependent stability for load frequency control with constant and time-varying delays," *IEEE Transactions on Power Systems*, vol. 27, no. 2, pp. 932-941, May 2012.

[9] D. K. Das, S. Ghosh, and B. Subudhi, "Tolerable delay-margin improvement for systems with input-output delays using dynamic delayed feedback controllers," *Applied Mathematics and Computation*, vol. 230, no. 1, pp. 57-64, Mar. 2014.

[10] R. Dey, S. Ghosh, G. Ray *et al.*, "H_∞ load frequency control of interconnected power systems with communication delays," *International Journal of Electrical Power & Energy Systems*, vol. 42, no. 1, pp. 672-684, Nov. 2012.

[11] X. Zhao, Y. Sun, N. Li *et al.*, "Robust H_∞ load frequency control of delayed multi-area power system with stochastic disturbances," *Neurocomputing*, vol. 193, pp. 58-67, Jun. 2016.

[12] X. Yu and K. Tomsovic, "Application of linear matrix inequalities for load frequency control with communication delays," *IEEE Transaction on Power Systems*, vol. 19, no. 3, pp. 1508-1515, Aug. 2004.

[13] L. Jiang, W. Yao, Q. H. Wu *et al.*, "Delay-dependent stability for load frequency control with constant and time-varying delays," in *Proceedings of IEEE PES General Meeting*, Calgary, Canada, Jul. 2009, pp. 1-6.

[14] M. Zribi, M.S. Mahmoud, M. Karkoub *et al.*, "H_∞ controllers for linearised time-delay power systems," *IEE Proceedings on Generation, Transmission and Distribution*, vol. 147, no. 6, pp. 401-408, Nov. 2000.

[15] C. Macana, E. Mojica-Nava, N. Quijano, "Time-delay effect on load frequency control for microgrids," in *Proceedings of IEEE International Conference on Networking, Sensing and Control (ICNSC)*, Evry, France, Apr. 2013, pp. 544-549.

[16] H. Shayeghi, A. Jalili, and H. A. Shayanfar, "A robust mixed based LFC of a deregulated power system including SMES," *Energy Conversion and Management*, vol. 49, no. 10, pp. 2656-2668, Oct. 2008.

[17] V. Donde, M. A. Pai, and I. A. Hiskens, "Simulation and optimization in an AGC system after deregulation," *IEEE Transaction on Power Systems*, vol. 16, no. 3, pp. 481-489, Aug. 2001.

[18] E. Rakhshani and J. Sadeh, "Practical viewpoints on load frequency control problem in a deregulated power system," *Energy Conversion and Management*, vol. 51, no. 6, pp. 1148-1156, Jun. 2010.

[19] H. Bevrani and T. Hiyama, "Practical robust decentralised PI based LFC design for time delay power systems," *Energy Conversion and Management*, vol. 49, no. 2, pp. 193-204, Feb. 2008.

[20] H. Bevrani and T. Hiyama, "On load-frequency regulation with time delays: design and real-time implementation," *IEEE Transactions on Energy Conversion*, vol. 24, no. 1, pp. 292-300, Mar. 2009.

[21] K. Vrdoljak, N. Peric, and I. Petrovic, "Sliding mode based load-frequency control in power systems," *Electric Power Systems Research*, vol. 80, no. 5, pp. 514-527, May 2010.

[22] H. Shayeghi, H.A. Shayanfar, and A. Jalili, "Multi-stage fuzzy PID power system automatic generation controller in deregulated environments," *Energy Conversion and Management*, vol. 47, no. 18, pp. 2829-2845, Nov. 2006.

[23] V. P. Singh, N. Kishor, and P. Samuel, "Communication time delay estimation for load frequency control in two-area power system," *Ad Hoc Networks*, vol. 41, no. 1, pp. 69-85, May 2016.

[24] M. Abu-Khalaf, J. Huang, and F.L. Lewis, *Nonlinear H2/H∞ Constrained Feedback Control: A Practical Design Approach Using Neural Networks*, London: Springer, 2006.

[25] H. Bevrani, M.R. Feizi, and S. Ataee, "Robust frequency control in an islanded microgrid: H_∞ and μ-synthesis approaches," *IEEE Transactions on Smart Grid*, vol. 7, no. 2, pp. 706-717, Mar. 2016.

[26] H. Liang, G. Li, G. Li *et al.*, "Analysis and design of H_∞ controller in VSC HVDC systems," in *Proceedings of IEEE PES Transmission & Distribution Conference & Exposition: Asia and Pacific*, Dalian, China, Aug. 2005, pp. 1-6.

[27] D. K. Das, "New results on delay-dependent stability analysis and stabilization of time-delay systems," Ph.D. thesis, Department of Electrical Engineering, National Institute of Technology Rourkela, Odisha, India, Jun. 2015.

[28] K. Gu and S. I. Niculescu, "Additional dynamics in transformed time-delay systems," *IEEE Transactions on Automatic Control*, vol. 45, no. 3, pp. 572-575, Mar. 2000.

[29] K. Gu, V. L. Kharitonov, and J. Chen, *Stability of Time-Delay Systems,* Boston: Birkhauser, 2003.

[30] E. Fridman and U. Shaked, "Input-output approach to stability and *L*2-gain analysis of systems with time-varying delays," *Systems and Control Letters*, vol. 55, no. 12, pp. 1041-1053, Dec. 2006.

[31] Q. L. Han, "A discrete delay decomposition approach to stability of linear retarded and neutral system," *Automatica*, vol. 45, no. 2, pp. 517-524, Feb. 2009.

[32] H. Bevrani and T. Hiyama, "Robust load-frequency regulation: a real-time laboratory experiment," *Optimal Control Applications and Methods*, vol. 28, no. 6, pp. 419-433, Nov. 2007.

[33] C. Briat, "Convergence and equivalence results for the Jensen's inequality application to time-delay and sampled-data systems," *IEEE Transactions on Automatic Control*, vol. 56, no. 7, pp. 1660-1665, Jul.

2011.
[34] H. Shao, “New delay-dependent stability criteria for systems with interval delay,” *Automatica*, vol. 45, no. 3, pp. 744-749, Mar. 2009.
[35] S. Boyd, L. E. Ghaoui, E. Feron *et al*., *Linear Matrix Inequalities in System and Control Theory*, vol. 15, Philadelphia: SIAM, 1994.
[36] D. D. Siljak, D. M. Stipanovic, and A. I. Zecevic, “Robust decentralized turbine/governor control using linear matrix inequalities,” *IEEE Transactions on Power Systems*, vol. 17, no. 3, pp. 715-722, Aug. 2002.
[37] D. D. Siljak and D. M. Stipanovic, “Robust stabilization of nonlinear systems: the LMI approach,” *Mathematical Problems in Engineering*, vol. 6, no. 5, pp. 461-493, Jun. 2000.

Subrat Kumar Pradhan received the B.Tech. degree in electrical engineering in 2012, and the M.Tech. degree in power system engineering in 2016, from Biju Patnaik University of Technology, Odisha, India. He is currently pursuing the Ph.D. degree in electrical and electronics engineering at National Institute of Technology Nagaland, Dimapur, India. His research interest includes the development of load frequency controllers for time-delay power systems using H_∞ control techniques.

Dushmanta Kumar Das received the B.Tech. degree in electronics and instrumentation engineering from Biju Patnaik University of Technology, Odisha, India, the M.Tech. and the Ph.D. degrees in control system engineering from National Institute of Technology Rourkela, Rourkela, India, in 2010 and 2015, respectively. Since 2013, he has been with National Institute of Technology Nagaland, Dimapur, India as an Assistant Professor. His research interests include time-delay system, control system, robotics, soft computing, machine learning, meta-heuristic optimization techniques and application of optimization techniques.